

# Preparation of I<sub>2</sub>@SWNTs: Synthesis and Spectroscopic Characterization of I<sub>2</sub>-Loaded SWNTs

Kyle R. Kissell,<sup>†</sup> Keith B. Hartman,<sup>†</sup> Paul A. W. Van der Heide,<sup>‡</sup> and Lon J. Wilson<sup>\*,†</sup>

Department of Chemistry, The R. E. Smalley Institute for Nanoscale Science and Technology, and the Center for Biological and Environmental Nanotechnology, MS-60, Rice University, P.O. Box 1892, Houston, Texas 77251-1892, and Center for Materials Chemistry, The University of Houston, 4800 Calhoun, Houston, Texas 77204

Received: February 11, 2006; In Final Form: July 3, 2006

X-ray photoelectron spectroscopy (XPS) along with inductively coupled plasma analysis (ICP-AE) and Raman spectroscopy have been used to define the location and to quantify the amount of iodine in HiPco SWNT samples loaded with molecular I<sub>2</sub> via sublimation (I<sub>2</sub>-SWNTs). The exterior-adsorbed I<sub>2</sub> can be removed (as I<sup>-</sup>) by reducing the sample of filled nanotubes with Na<sup>0</sup>/THF or by heating the I<sub>2</sub>-SWNTs to 300 °C (without reduction), leaving I<sub>2</sub> contained only within the interior of the SWNTs (I<sub>2</sub>@SWNTs) as proven by XPS. These I<sub>2</sub>@SWNTs contain ~25 wt % of I<sub>2</sub> and are stable without the loss of I<sub>2</sub> even after exposure to additional reduction with Na<sup>0</sup>/THF or upon heating to ca. 500 °C.

## Introduction

A central question surrounding filled single-walled carbon nanotubes (SWNTs)<sup>1</sup> is whether the filling material is contained within the interior of the SWNT or adsorbed to its exterior surface. Nanotubes aggregate into large bundles which are difficult to separate (~1 eV/nm binding energy)<sup>2</sup> and hydrophobic molecules, e.g., I<sub>2</sub>, can become intercalated in the surface spaces within a nanotube bundle. For many potential applications, especially those in the medical field involving toxic ions (e.g. Gd<sup>3+</sup> for MRI imaging) and molecules (e.g. I<sub>2</sub> for CT imaging), it is necessary to not only distinguish between the intercalated and internally loaded agent, but to also remove all exterior-adsorbed material, leaving only internally loaded SWNTs. Previous work involving filling SWNT samples has primarily focused on exploring the various methods of filling SWNTs with an assortment of molecules.<sup>1,3–8</sup> For example, Eklund and co-workers reported the filling of SWNTs with molten iodine, producing SWNTs loaded with polyiodide chains (I<sub>3</sub><sup>-</sup> and I<sub>5</sub><sup>-</sup>).<sup>4,5</sup> In this work, we report the filling of SWNTs with I<sub>2</sub> via sublimation, a procedure that has previously been shown to produce the highest filling yield.<sup>8</sup> Virtually all previous research about filling SWNT samples has been performed with electric-arc discharge-produced SWNTs because arc-produced SWNTs have a larger diameter than HiPco SWNTs (1.4 nm average diameter for arc vs 1.0 nm diameter for HiPco) and arc SWNTs are generally believed to contain more sidewall defects than HiPco SWNTs. For medical applications, however, the uniformity and purity of HiPco SWNTs is advantageous, thus this work was performed solely with HiPco SWNTs. Because HiPco produced SWNTs are not typically used for filling experiments (the vast majority of previous research has been performed on arc-produced SWNTs), we believed that the interior of a HiPco SWNT was inaccessible for filling due to the lack of sidewall defects and the presence of the iron catalyst particle which often blocks the open end of the SWNT.

However, we show below that HiPco SWNTs do, indeed, fill readily with I<sub>2</sub>, without prior exposure to strong acids which are known to create sidewall defects.<sup>7,10</sup> The mechanism behind this filling is unknown, although one possible explanation could be that I<sub>2</sub> first reacts with the iron catalyst particle to remove it from the SWNT, thus allowing filling through the now open end of the SWNT. Thermal gravimetric analysis (TGA) in air supports this speculation, since the residual mass (due to the presence of iron oxide formed during combustion of the sample) of an I<sub>2</sub>-SWNT sample is significantly less when compared to a raw SWNT sample (Supporting Information).

Previous work involving filled SWNTs primarily has used super-resolved high resolution transmission electron microscopy (HRTEM) to characterize the filled SWNTs. However, this requires a modified instrument that is not available in most laboratories. Additionally, TEM only analyzes a small portion of a bulk sample and is very time-consuming. For these reasons, spectroscopic techniques are also desirable for thorough characterization of filled SWNT materials. Here, we present a procedure to fill HiPco SWNT samples with I<sub>2</sub> in high yield via sublimation and for the subsequent removal of all exterior-adsorbed I<sub>2</sub>, leaving only internally loaded SWNTs (I<sub>2</sub>@SWNTs) as established spectroscopically. In addition, X-ray photoelectron spectroscopy (XPS) and inductively coupled plasma analysis (ICP-AE) have been used to characterize these internally loaded SWNTs by defining the location and quantifying the amount of loading material in the specific case of I<sub>2</sub>@SWNTs.

## Experimental Methods

A raw nanotube sample, produced by the HiPco process,<sup>9</sup> with an average diameter of 1.0 nm and containing ~35 wt % iron catalyst impurities was obtained from Carbon Nanotechnologies Inc. The, as received, sample was not purified by exposure to a strong acid treatment which is known to create additional defects in the sidewalls.<sup>7,10</sup>

Filling of a SWNT sample was accomplished by sublimation of I<sub>2</sub> (~100 °C) in the presence of SWNTs for 1 h in a closed glass vessel. Previous experiments<sup>3,4,7</sup> have shown sublimation

\* Address correspondence to this author. E-mail: durango@rice.edu.

<sup>†</sup> Rice University.

<sup>‡</sup> The University of Houston.

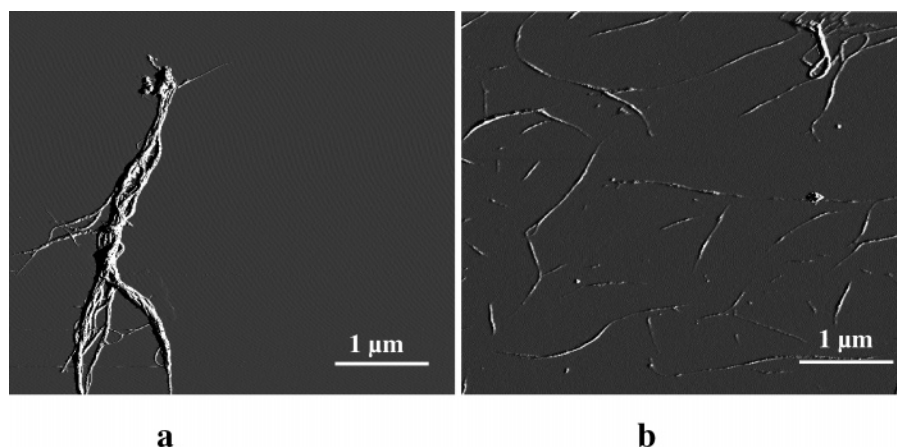


**Figure 1.** AFM image of (a) raw HiPco SWNTs and (b) Na<sup>0</sup>/THF reduced HiPco SWNTs.

to be the most efficient method for filling SWNTs, producing near 100% yields in the case of “C<sub>60</sub>-peapod” formation.<sup>8</sup> In a typical experiment, 50 mg of raw SWNTs were used and the SWNT sample gained approximately 80% mass during the filling process (total mass after filling was ~90 mg). XPS spectra were obtained for samples untreated after filling (hereafter I<sub>2</sub>-SWNTs), and for I<sub>2</sub>-SWNT samples which were reduced with sodium metal in dry tetrahydrofuran (THF). The reduction reaction results in the SWNTs becoming highly charged (~10 electrons/nm), which creates an electrostatic repulsion resulting in the debundling of the nanotubes into mostly individual SWNTs.<sup>11</sup> This debundling allows for any I<sub>2</sub>, which is intercalated within the surface spaces of a SWNT bundle, to be chemically reduced to I<sup>-</sup> and washed away. In a typical experiment, 50 mg of I<sub>2</sub>-SWNTs was added to a dry 250 mL round-bottom flask with a 2:1 molar excess of sodium metal (100 mg). Then, 150 mL of dry THF was added to the flask, and the flask was purged with N<sub>2(g)</sub>, capped, and bath sonicated for 1 h. After 1 h, the reduction reaction was quenched with DI water and the sample was isolated with a glass frit filter (Pyrex No. 36060). The THF/water filtrate was heated to remove the THF and ICP-AE was performed to quantify the amount of iodine (as NaI) removed during the reduction reaction.

To ensure complete removal of exterior-adsorbed I<sub>2</sub> and to assess the stability of the internal I<sub>2</sub>, a second Na<sup>0</sup>/THF reduction was performed under the same conditions. The resulting, twice-reduced I<sub>2</sub>@SWNTs were analyzed by XPS and ICP. Variable-temperature XPS studies, under high vacuum to prevent combustion of the SWNTs, were also performed on the I<sub>2</sub>-SWNTs to compare the thermal stability of the internal I<sub>2</sub> vs external I<sub>2</sub>.

XPS analysis was performed with a Physical Electronics Model 5700 XPS instrument with photo and Auger emissions produced via a monochromatic Al K $\alpha$  X-ray source (1486.6 eV) operated at 350 W. All emissions were acquired at takeoff angles ranging from 10° to 70° as defined relative to the surface plane. The signals were passed through a hemispherical analyzer operated at a pass energy of 11.75 eV. The area analyzed and the collection solid cone were fixed at 800  $\mu$ m and 5°, which results in an energy resolution of  $\leq 0.51$  eV. Charge neutralization was ensured through co-bombardment of the analyzed area with a low-energy electron beam.

Inductively coupled plasma analysis with an atomic emission detector (ICP-AE) was performed with a Varian Vista Pro Simultaneous Axial Inductively Coupled Atomic Emission Spectrometer with an atomic emission CCD detector. A calibration curve was generated by using 50, 100, 250, 500, and 1000

ppm I<sup>-</sup> standards and 10 replicates were collected for each sample, resulting in a relative standard deviation of <2%.

Raman spectroscopy was performed with a Renishaw micro-Raman spectrometer operating with a 780 nm laser and a 1200 L/mm grating. Atomic force microscopy (AFM) was performed on a Digital Instruments multimode microscope operated in tapping mode; the SWNT samples were first suspended in water via sonication, then spin-coated onto mica for imaging. Mass spectrometry data were acquired with a Bruker Biflex III MALDI-TOF mass spectrometer.

## Results and Discussion

Before experiments on I<sub>2</sub>-SWNTs were performed, the effects of the Na<sup>0</sup>/THF reduction reaction on raw SWNTs were measured. Atomic force microscopy (AFM) confirmed the debundling of the raw SWNTs by the Na<sup>0</sup>/THF reduction reaction into mostly individuals (Figure 1). The AFM image was acquired before the addition of water, although the SWNTs were likely quenched via exposure to the atmosphere. Height measurements taken for several points in the reduced SWNT sample measured ~1 nm, corroborating individual SWNTs (Supporting Information).

Raman spectroscopy has been used to assess structural changes in the raw SWNTs as a result of the Na<sup>0</sup>/THF reduction reaction. Such changes could be either residual delocalized negative charge not quenched by the addition of water, or protonation (similar to the Birch reaction)<sup>12,13</sup> of the charged SWNTs upon quenching by water. As shown in Figure 2, the Raman spectra before and after reduction are nearly identical, with the exception of a small increase in the disorder band at ~1300 cm<sup>-1</sup>. This band is indicative of sp<sup>3</sup>-hybridized carbons, which suggests that some degree of protonation of the SWNTs has occurred.

After filling, the I<sub>2</sub>-SWNTs contained 5.3 atomic % of iodine by XPS (36 wt %), which agrees well with the mass gain observed during the filling process. The position of the I-3d<sub>5/2</sub> peak in the XPS spectrum at 619.5  $\pm$  0.2 eV is consistent with accepted values for I<sub>2</sub> (as opposed to polyiodide chains such as I<sub>3</sub><sup>-</sup> and I<sub>5</sub><sup>-</sup>),<sup>14</sup> indicating that I<sub>2</sub> does not react with SWNTs to form C–I bonds. This is also confirmed by the absence of a second peak in the C 1s spectrum of the I<sub>2</sub>-SWNT sample (Supporting Information).

After an I<sub>2</sub>-SWNT sample was reduced by the Na<sup>0</sup>/THF reaction, 2.8 atomic % or 22 wt % I<sub>2</sub> remained in the sample, which approximates to be 3.1 atoms of iodine/nm of SWNT. This value is calculated by using the relative atomic percentages of carbon and iodine, as measured by XPS, based on an

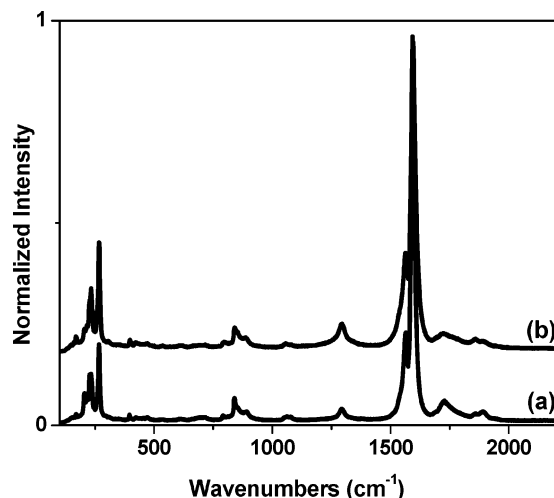


**Figure 2.** Raman spectrum of (a) raw HiPco SWNTs and (b) Na<sup>0</sup>/THF reduced HiPco SWNTs.

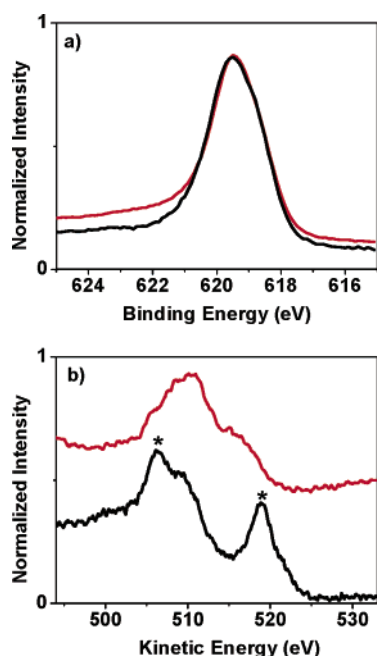


**Figure 3.** (a) I 3d<sub>5/2</sub> XPS spectrum of I<sub>2</sub>-SWNTs (black) and I<sub>2</sub>@SWNTs (red) reduced by the Na<sup>0</sup>/THF reaction and then quenched by water. (b) X-ray induced Auger emission spectrum over the IMNN region for I<sub>2</sub>-SWNTs (black) and I<sub>2</sub>@SWNTs (red) reduced by the Na<sup>0</sup>/THF reaction and then quenched by water. The peaks due to externally adsorbed I<sub>2</sub> are denoted by an asterisk.

assumption of 100 carbons per nm of SWNT. A slight shift of the I-3d<sub>5/2</sub> peak to a lower binding energy ( $619.1 \pm 0.2$  eV) was observed in the reduced I<sub>2</sub>@SWNT sample; however, the shift is within experimental error and is not large enough to provide conclusive evidence as to the removal of exterior-adsorbed I<sub>2</sub>. Additionally, this value is still within those accepted for I<sub>2</sub>, which indicates the remaining I<sub>2</sub> in the sample has not been reduced to some polyiodide form (I<sub>3</sub><sup>-</sup> or I<sub>5</sub><sup>-</sup>). This would likely occur only if the remaining I<sub>2</sub> was sequestered within the interior of the hydrophobic nanotube and, therefore, inaccessible to chemical reduction. Representative XPS spectra comparing an I<sub>2</sub>-SWNT sample and a Na<sup>0</sup>/THF reduced I<sub>2</sub>@SWNT sample in the I-3d<sub>5/2</sub> region are shown in Figure 3, panels a and b, respectively.

Inspection of the X-ray induced iodine Auger emissions (these form as a result of the core hole produced on photoelectron

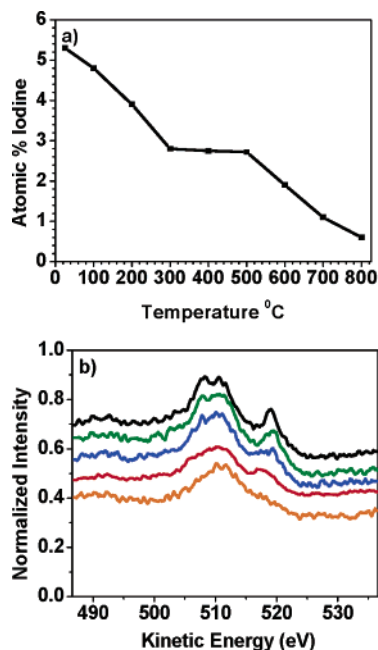


**Figure 4.** (a) Variable-temperature XPS study of I<sub>2</sub>-SWNTs under high vacuum and (b) X-ray induced Auger emission spectrum of I<sub>2</sub>-SWNTs at room temperature (black), at 100 °C (green), at 200 °C (blue), at 300 °C (red), and reduced by the Na<sup>0</sup>/THF reduction reaction (yellow). All spectra were acquired under high vacuum. Possible instrument error in part a is  $\pm 10$  °C and  $\pm 0.1\%$  iodine.

emission)<sup>15</sup> reveals differences between the I<sub>2</sub>-SWNT sample and the Na<sup>0</sup>/THF reduced I<sub>2</sub>@SWNTs. In short, the unreduced I<sub>2</sub>-SWNT sample exhibits peaks at kinetic energies of  $507.5 \pm 0.2$  and  $519.0 \pm 0.2$  eV. Additionally, there is a prominent shoulder observed on the 507.5 eV peak, with a maximum at  $\sim 510$  eV. The reduced I<sub>2</sub>@SWNT sample on the other hand exhibits a single peak at  $510.0 \pm 0.2$  eV with a shoulder at approximately 517 eV. This shoulder was hidden by the external I<sub>2</sub> peak at 519 eV and is likely also due to internal I<sub>2</sub>. This phenomenon is also observed in the Auger temperature studies discussed below (red trace in Figure 4b). The 507.5 and 510.0 eV peaks stem from I-M<sub>5</sub>N<sub>45</sub>N<sub>45</sub> emissions, whereas the 519.0 eV peak stems from I-M<sub>4</sub>N<sub>45</sub>N<sub>45</sub> emissions.<sup>15</sup> Representative spectra comparing the iodine photoelectron and X-ray induced Auger emissions for the I<sub>2</sub>-SWNT (black) and reduced I<sub>2</sub>@SWNT (red) samples are shown in Figure 3.

Since the I-M<sub>4</sub>N<sub>45</sub>N<sub>45</sub> emissions appear at 11.5 eV lower kinetic energy than I-M<sub>5</sub>N<sub>45</sub>N<sub>45</sub> emissions,<sup>15</sup> addition of this value allows for Auger parameters to be derived. Such parameters are an effective method of deriving additional chemical state information.<sup>15</sup> Auger parameters are derived by adding the I-3d<sub>5/2</sub> peak binding energy to the I-M<sub>4</sub>N<sub>45</sub>N<sub>45</sub> kinetic energy, or by adding the I-3d<sub>5/2</sub> peak binding energy to the I-M<sub>5</sub>N<sub>45</sub>N<sub>45</sub> kinetic energy plus 11.5 eV. For the unreduced I<sub>2</sub>-SWNT sample, Auger parameter values of 1138.5 eV for the 507.5 eV peak, 1141.0 eV for the 510.0 eV shoulder, and 1138.5 eV for the 519.0 eV peak are derived. A value of 1141.0 eV is derived for the peak at 510.0 eV in the Na<sup>0</sup>/THF reduced I<sub>2</sub>@SWNT sample.

The Auger peak at 510.0 eV is thus assigned to internally loaded I<sub>2</sub>, while those at 507.5 and 519.0 eV are attributed to externally adsorbed I<sub>2</sub>. The difference in the kinetic energies of these Auger emissions represents a definitive method of distinguishing between internal and external I<sub>2</sub>. Auger parameters of 1138 eV are consistent with I<sub>2</sub>,<sup>15</sup> confirming once again that the external-adsorbed iodine is I<sub>2</sub>, not a polyiodide or a



C–I species. The shift observed in the Auger parameter, from 507.5 to 510.0 eV, for internal  $I_2$ , is likely due to the unique chemical environment experienced by  $I_2$  confined within the interior of a SWNT.

ICP-AE confirmed the presence of iodine (present as NaI) in the filtrate after the reduction reaction. A 20 mL aliquot (total volume of filtrate is  $\sim 35$  mL) contained 550 mg/L of  $I^-$ , which corresponds to a total mass of  $\sim 20$  mg of  $I_2$  removed from the  $I_2$ -SWNT sample during the reduction reaction. This is consistent with the change observed in the atomic percent of  $I_2$  by XPS.

After a second  $Na^0/THF$  reduction, 2.3 atomic % of iodine remained, which is unchanged (within error) from the amount of  $I_2$  present in the  $I_2$ -SWNT sample after the first reduction. Additionally, the peak positions for iodine in the XPS spectra were unchanged from the positions after the first reduction. ICP-AE also confirmed that no iodine (as NaI) was present in the filtrate after the second reduction. This established that internal  $I_2$  is truly sequestered within the interior of the nanotube ( $I_2@SWNTs$ ) and is impervious to chemical reduction by  $Na^0/THF$ .

Variable-temperature XPS analysis was performed on an  $I_2$ -SWNT sample to assess the thermal stability of the internal vs external  $I_2$ . A sample of the unreduced  $I_2$ -SWNTs was heated from room temperature to 800 °C under high vacuum. During this process, a mass spectrum analysis indicated  $I_2^+$  (254 amu) and  $I^+$  (127 amu) were the only positive ion species liberated from the  $I_2$ -SWNT sample in the temperature range of 200–800 °C. XPS spectra and X-ray induced Auger emission spectra were acquired every 100 °C. As shown in Figure 4, a linear loss of iodine was observed by XPS from room temperature until 300 °C. From 300 to 500 °C, the iodine content remained constant, and above 500 °C linear loss was again observed. The atomic percent of iodine remaining at 400 °C was  $\sim 2.6\%$ , a value consistent with the amount of internally loaded  $I_2$  from the reduction experiments. As also shown in Figure 4, the Auger emission spectra of the  $I_2$ -SWNTs at room temperature (black), 100 °C (green), 200 °C (blue), 300 °C (red), and after the  $Na^0/THF$  reduction reaction (yellow) confirmed that the decrease in the atomic percent of iodine observed by XPS is due to the removal of exterior-adsorbed  $I_2$ . The Auger peaks at 507.5 and 519.0 eV, assigned above to externally adsorbed  $I_2$ , decreased in intensity from room temperature until their disappearance at  $\sim 300$  °C. This is illustrated by the shift from an unresolved doublet in the 505–510 eV region at room temperature (black trace in Figure 4b, maxima at 507.5 and 510 eV) to a single peak at 300 °C (red trace in Figure 4b, maximum at 510 eV). As discussed above, a shoulder is once again observed at  $\sim 517$  eV after the external  $I_2$  is removed from the SWNT sample (red trace in Figure 4b). The Auger peak at 510.0 eV, assigned to internal  $I_2$ , was largely unchanged during the temperature study. The spectrum of  $I_2$ -SWNTs at 300 °C (red trace in Figure 4b) and the spectrum for reduced  $I_2$ -SWNTs (yellow trace in Figure 4b) are identical with respect to the features at 507.5 and 519.0 eV. Heating to 300 °C thus provides an alternative method for removing externally adsorbed  $I_2$ . It is possible to also remove the interior  $I_2$  from the SWNT sample, but temperatures upward of 800 °C are required.

Finally, Raman spectroscopy has been used to identify the I–I stretching mode which should be present in the  $I_2$ -SWNT sample. As shown in Figure 5, there was an additional band at  $152\text{ cm}^{-1}$  in the Raman spectrum of  $I_2$ -SWNTs (b) which was not present in the raw SWNT spectrum (a). This band is therefore assigned to the  $\nu(I-I)$  stretching mode. Interestingly,

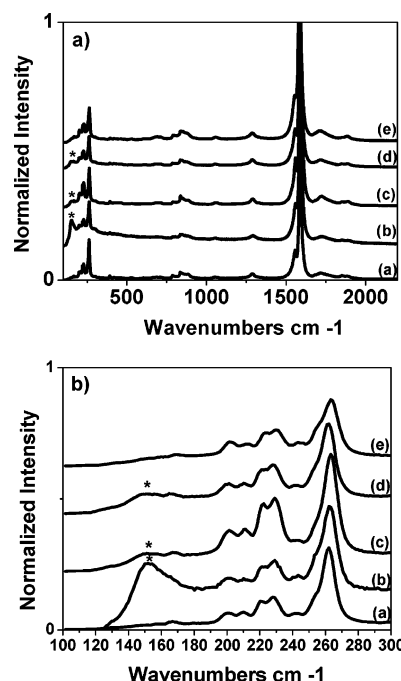


**Figure 5.** (a) Raman spectrum of (a) raw SWNTs, (b)  $I_2$ -SWNTs, (c)  $Na^0/THF$  reduced  $I_2$ -SWNTs, (d)  $I_2$ -SWNTs heated to 400 °C, and (e)  $I_2$ -SWNTs heated to 1000 °C. (b) The low energy region of panel a magnified. The  $\nu(I-I)$  stretching mode peak is denoted by an asterisk.

this  $\nu(I-I)$  stretching mode decreased significantly when the  $I_2$ -SWNTs were reduced by the  $Na^0/THF$  reduction reaction or heated to 400 °C (Figure 5, spectra c and d, respectively). Upon heating to 1000 °C, which removes all  $I_2$  according to XPS, the  $152\text{ cm}^{-1}$  band completely disappeared (Figure 5, spectrum e) and the Raman spectrum was once again identical to that for the raw SWNT sample (Figure 5a).

## Conclusions

Filling of HiPco SWNTs with  $I_2$  in high yield has been performed by sublimation with  $I_2$  and the subsequent removal of all exterior-adsorbed  $I_2$  has been achieved. Exterior  $I_2$  can be removed by either reducing the filled SWNTs with  $Na^0/THF$  or by heating to 300 °C under high vacuum without the chemical reduction step. The resulting internally loaded SWNTs or  $I_2@SWNTs$  contain  $\sim 25$  wt %  $I_2$ , which is remarkably stable toward additional chemical reduction or elevated temperatures. Although XPS is effective in quantifying the amount of  $I_2$  present, Auger parameters are necessary to distinguish between externally adsorbed and internally loaded  $I_2$  in a  $I_2$ -SWNT sample. Raman spectroscopy can also be used to discriminate between internal and external  $I_2$ , by way of the relative intensities of the  $\nu(I-I)$  stretching mode, but only in conjunction with XPS spectral data. Future studies will concentrate on analogous ultra-short  $I_2$ -US-tube and  $I_2@US$ -tube species<sup>16,17</sup> as potential X-ray contrast agents for biological and medical imaging applications.

**Acknowledgment.** This work was supported by the Robert A. Welch Foundation (Grant C-0627), Carbon Nanotechnologies Inc. (Houston, Texas), and NASA Johnson Space Center and University of Texas Health Science Center (Grant NNJ05HE75A).

**Supporting Information Available:** Thermal gravimetric analysis (TGA) in air of raw SWNTs and  $I_2$ -SWNTs (Figure S-1), atomic force microscopy height measurements of raw HiPco SWNTs (Figure S-2), atomic force microscopy height

measurements of Na<sup>0</sup>/THF reduced HiPco SWNTs (Figure S-3), and carbon 1s XPS spectrum for I<sub>2</sub>-SWNTs (Figure S-4). This material is available free of charge via the Internet at <http://pubs.acs.org>.

## References and Notes

- (1) Ugarte, D.; Stoeckli, T.; Bonard, J. M.; Chatelain, A.; De Heer, W. A. *Appl. Phys. A: Mater. Sci. Process.* **1998**, *A67*, 101–105.
- (2) O'Connell, M. J.; Boul, P.; Ericson, L. M.; Huffman, C.; Wang, Y.; Haroz, E.; Kuper, C.; Tour, J.; Ausman, K. D.; Smalley, R. E. *Chem. Phys. Lett.* **2001**, *342*, 265–271.
- (3) Brown, G.; Bailey, S. R.; Novotny, M.; Carter, R.; Flahaut, E.; Coleman, K. S.; Hutchison, J. L.; Green, M. L. H.; Sloan, J. *Appl. Phys. A: Mater. Sci. Process.* **2003**, *76*, 457–462.
- (4) Fan, X.; Dickey, E. C.; Eklund, P. C.; Williams, K. A.; Grigorian, L.; Buczko, R.; Pantelides, S. T.; Pennycook, S. J. *Phys. Rev. Lett.* **2000**, *84*, 4621–4624.
- (5) Grigorian, L.; Williams, K. A.; Fang, S.; Sumanasekera, G. U.; Loper, A. L.; Dickey, E. C.; Pennycook, S. J.; Eklund, P. C. *Phys. Rev. Lett.* **1998**, *80*, 5560–5563.
- (6) Hutchison, J. L.; Sloan, J.; Dunin-Borkowski, R.; Kirkland, A. I.; Green, M. L. H. *Sci. Technol. Nanostruct. Mater. [Pap. Int. Conf.]* **2001**, 143–149.
- (7) Sloan, J.; Hammer, J.; Zwiefka-Sibley, M.; Green, M. L. H. *Chem. Commun. (Cambridge, U.K.)* **1998**, 347–348.
- (8) Smith, B. W.; Russo, R. M.; Chikkannanavar, S. B.; Luzzi, D. E. *J. Appl. Phys.* **2002**, *91*, 9333–9340.
- (9) Bronikowski, M. J.; Willis, P. A.; Colbert, D. T.; Smith, K. A.; Smalley, R. E. *J. Vac. Sci. Technol., A* **2001**, *19*, 1800–1805.
- (10) Mawhinney, D. B.; Naumenko, V.; Kuznetsova, A.; Yates, J. T.; Liu, J.; Smalley, R. E. *Chem. Phys. Lett.* **2000**, *324*, 213–216.
- (11) Penicaud, A.; Poulin, P.; Derre, A.; Anglaret, E.; Petit, P. *J. Am. Chem. Soc.* **2005**, *127*, 8–9.
- (12) Liang, F.; Sadana, A. K.; Gu, Z.; Peera, A.; Chattopadhyay, J.; Kittrell, C.; Hauge, R. H.; Smalley, R. E.; Billups, W. E. *Abstracts*; 60th Southwest Regional Meeting of the American Chemical Society, Fort Worth, TX, September 29–October 4, 2004; SEPT04-195.
- (13) Pekker, S.; Salvétat, J. P.; Jakab, E.; Bonard, J. M.; Forro, L. *J. Phys. Chem. B* **2001**, *105*, 7938–7943.
- (14) Wagner, C. D. In *NIST technical note*, 1289; U.S. Department of Commerce, National Institute of Standards and Technology: Gaithersburg, MD, 1991.
- (15) Briggs, D.; Seah, M. P.; Editors *Practical Surface Analysis by Auger and X-ray Photoelectron Spectroscopy*; Wiley: New York, 1983.
- (16) Mackeyev, Y. A.; Marks, J. W.; Rosenblum, M. G.; Wilson, L. J. *J. Phys. Chem. B* **2005**, *109*, 5482–5484.
- (17) Sitharaman, B.; Kissell, K. R.; Hartman, K. B.; Tran, L. A.; Baikarov, A.; Rusakova, I.; Sun, Y.; Khant, H. A.; Ludtke, S. J.; Chiu, W.; Laus, S.; Toth, E.; Helm, L.; Merbach, A. E.; Wilson, L. J. *Chem. Commun. (Cambridge, U.K.)* **2005**, 3915–3917.